Atmos. Meas. Tech. Discuss., 8, 8563–8597, 2015
www.atmos-meas-tech-discuss.net/8/8563/2015/
doi:10.5194/amtd-8-8563-2015

Atmospheric Measurement Techniques Discussions

Space-borne observation of methane from atmospheric infrared sounder version 6: validation and implications for data analysis

X. Xiong[1,2], **F. Weng**[2], **Q. Liu**[2], **and E. Olsen**[3]

[1]Earth Resources Technology Inc., Laurel, MD 20707, USA
[2]NOAA Center for Satellite Applications and Research, College Park, MD 20740, USA
[3]NASA/Jet Propulsion Laboratory, Pasadena, CA, USA

Received: 12 June 2015 – Accepted: 22 July 2015 – Published: 10 August 2015

Correspondence to: X. Xiong (xiaozhen.xiong@noaa.gov)

Published by Copernicus Publications on behalf of the European Geosciences Union.

Abstract

Atmospheric Methane (CH_4) is generated as a standard product in recent version of the hyperspectral Atmospheric Infrared Sounder (AIRS-V6) aboard NASA's Aqua satellite at the NASA Goddard Earth Sciences Data and Information Services Center (NASA/GES/DISC). Significant improvements in AIRS-V6 was expected but without a thorough validation. This paper first introduced the improvements of CH_4 retrieval in AIRS-V6 and some characterizations, then presented the results of validation using ~1000 aircraft profiles from several campaigns spread over a couple of years and in different regions. It was found the mean biases of AIRS CH_4 at layers 343–441 and 441–575 hPa are −0.76 and −0.05 % and the RMS errors are 1.56 and 1.16 %, respectively. Further analysis demonstrates that the errors in the spring and in the high northern latitudes are larger than in other seasons or regions. The error is correlated with Degree of Freedoms (DOFs), particularly in the tropics or in the summer, and cloud amount, suggesting that the "observed" spatiotemporal variation of CH_4 by AIRS is imbedded with some artificial impact from the retrieval sensitivity in addition to its variation in reality, so the variation of information content in the retrievals needs to be taken into account in data analysis of the retrieval products. Some additional filtering (i.e. rejection of profiles with obvious oscillation as well as those deviating greatly from the norm) for quality control is recommended for the users to better utilize AIRS-V6 CH_4, and their implementation in the future versions of the AIRS retrieval algorithm is under consideration.

1 Introduction

Atmospheric methane (CH_4) is not only an important greenhouse gases (GHGs) but also plays an important role in atmospheric chemistry. As a GHG, it plays 25 times more effective on a per unit mass basis than CO_2 in absorbing long-wave radiation on a 100-year time horizon (IPCC, 2007). The reaction of CH_4 with hydroxyl radicals

AMTD
8, 8563–8597, 2015

(OH) produces CH_3 and water, and the removal of OH via this reaction significantly impacts many other oxidation processes related with OH in the atmosphere. It is found that the concentration of CH_4 in the atmosphere has increased from the pre-industrial levels of about 700 parts per billion (ppb) to about 1800–1900 ppb, and this increase is mainly attributed to the impact of human activities. However, the increase rate of CH_4 is not stable, and after remaining stable for over a decade, a rapid increase has been observed beginning in 2007. The causes of this increase are the focus of many recent studies (e.g., Bousquet et al., 2011; Bergamaschi et al., 2013; Bruhwiler et al., 2014), and more observations are required.

Systematic high-precision measurements of CH_4 mixing ratios and the CH_4 isotope ratios have been made for over 25 years by taking the air samples near the ground and measuring the concentration in the laboratory (e.g. Chen and Prinn, 2006; Bousquet et al., 2006, 2011), which include the measurements at the sites of NOAA/ESRL/GMD (National Oceanic and Atmospheric Administration, Earth System Research Laboratory, Global Monitoring Division) networks and other sites under the umbrella of the WMO (World Meteorological Organization) Global Atmosphere Watch (GAW) programme. Another type of measurements with a good data record is the ground-based remote sensing using solar Fourier-transform-spectrometry (FTS) instruments, which provide measurements of the total column amount of CH_4, and these data are available from the Network for the Detection of Atmospheric Composition Change (NDACC) (http://www.ndsc.ncep.noaa.gov/). The vertical variation of CH_4 in the atmosphere was measured in recent years using aircrafts, and most of them were made especially over North America. One usage of these data is to validate satellite remote sensing observations (see Xiong et al., 2010, 2013a and references therein).

Recent improvements in satellite sensors, particularly the increase of spectral resolution, made the space-borne measurements of CH_4 from satellites possible. One class of instrument uses thermal infrared (TIR) sensors, such as the AIRS on NASA/AQUA (Aumann et al., 2003; Xiong et al., 2008, 2010), the Tropospheric Emission Spectrometer (TES) on NASA/Aura (Payne et al., 2009; Wecht et al., 2012; Worden et al., 2012;

AMTD
8, 8563–8597, 2015

Alvarado et al., 2015), and the Infrared Atmospheric Sounding Interferometer (IASI) on METEOP-A and METEOP-B (Crevoisier et al., 2009, 2013; Razavi et al., 2009; Xiong et al., 2013a). Another class of instrument employs Near-Infrared (NIR) sensors, such as the SCanning Imaging Absorption spectroMeter for Atmospheric CHartography (SCIAMACHY) instrument onboard ENVISAT for 2003–2009 (e.g. Frankenberg et al., 2008, 2011), and the Thermal And Near infrared Sensor for carbon Observation (TANSO) onboard the Greenhouse gases Observation SATellite (GOSAT) from 2009–present (Yokota et al., 2009; Park et al., 2011; Schepers et al., 2012; Saitoh et al, 2012). These satellite sensors provide a complementary measurement to surface and airborne observations of atmospheric CH_4 with a large spatial and temporal coverage (Kirschke et al., 2013). Combining the surface and satellite measurements allows inverse modeling to better constrain the quantification of CH_4 sources and sinks in different time and space domain (e.g. Meirink et al., 2008; Bergamaschi et al., 2013; Houwelling et al., 2014; Massart et al., 2014). For example, Massart et al. (2014) assimilated SCIAMACHY, GOSAT/TANSO, IASI and a combination of TANSO and IASI CH_4 products in the Monitoring Atmospheric Composition and Climate Interim Implementation (MACC-II) system to produce the atmospheric CH_4 analysis in about 6 months behind real time. Using the four-dimensional variational (4DVAR) inverse modeling system TM5-4DVAR and data of the surface observations during 2000–2010 from NOAA/ESRL/GMD network together with retrievals of column-averaged CH_4 mole fractions from SCIAMACHY, Bergamaschi et al. (2013) found that the global total emissions for 2007–2010 are 16–20 Tg CH_4 yr^{-1} higher compared to 2003–2005, and that most of the inferred emission increase was located in the tropics (9–14 Tg CH_4 yr^{-1}) and mid-latitudes of the northern hemisphere (6–8 Tg CH_4 yr^{-1}). Using the CarbonTracker-CH_4 assimilation system but the surface observation data only, Bruhwiler et al. (2014) estimated emissions from natural sources in 2007 were greater than the decadal average by 4.4 ± 3.8 Tg CH_4 yr^{-1}.

The benefit of satellite data in inverse modeling is limited by the uncertainty in both the satellite data and the transport model. As pointed out by Houwelling et al. (2014),

AMTD
8, 8563–8597, 2015

assimilating SCIAMACHY retrievals into TM5 4DVAR increases the estimated inter-annual variability of large-scale fluxes by 22 % as compared to that resulting from assimilating only surface observations, and systematic errors in the SCIAMACHY measurements are a main factor limiting the performance of the inversions. Therefore validation of the satellite retrieval products to quantify their accuracy and precision is very important to facilitate their use in inverse modeling, and at the same time, it is one essential step for further improvement of the retrieval algorithms.

As a stable TIR sensor, AIRS has been used to retrieve temperature and water vapor profiles as well as some trace gases since 2002. Xiong et al. (2008) described the characterization and some validation of AIRS-V5 CH_4 product. Some significant improvements are expected for AIRS-V6 temperature and water vapor retrieval products as well as trace gases. This study is the first one to systematically evaluate the quality of the AIRS-V6 CH_4 product using in-situ aircraft profiles. Section 2 provides a brief summary of the CH_4 retrieval improvements in AIRS-V6 and its sensitivity. Section 3 describes the validation data and method. Based on these validations, some optimization of quality control (QC) is recommended. Section 4 provides the validation results and error analysis. The summary of results and conclusions are given in Sect. 5.

2 Improvements in CH_4 retrieval in AIRS-V6 and averaging kernels

2.1 AIRS and improvement in AIRS-V6 CH_4 retrieval

AIRS was launched in polar orbit (13:30 local solar time, ascending node) on the EOS/Aqua satellite in May 2002. It has 2378 channels covering 649–1136, 1217–1613 and 2169–2674 cm^{-1} at high spectral resolution ($\lambda/\Delta\lambda = 1200$) (Aumann et al., 2003). The spatial resolution of the AIRS field-of-view (FOV) is 13.5 km at nadir, and in a 24-h period AIRS nominally observes the complete globe twice per day. In order to retrieve CH_4 in both clear and partial cloudy scenes, a 3×3 array of 9 AIRS FOVs within the footprint of the Advanced Microwave Sounding Unit (AMSU) is used

AMTD
8, 8563–8597, 2015

to derive a single cloud-cleared radiance spectrum in a field-of-regard (FOR), which is then used for retrieving profiles with a spatial resolution of about 45 km. The AIRS retrieval algorithm is a sequential retrieval with multiple steps, in which the temperature and water vapor profiles, surface temperature and surface emissivity are retrieved first using channel subsets optimized for the component being retrieved. Thus the CH_4 retrieval in version 6 benefited from the AIRS science team's efforts to improve the temperature and moisture profiles and their quality control (e.g. Susskind et al., 2011; Maddy et al., 2012). AIRS data used in this study were downloaded from the NASA Goddard Earth Sciences Data and Information Services Center (DISC) (http://disc.sci.gsfc.nasa.gov/AIRS/data-holdings/by-data-product-V6).

For CH_4 retrieval, the upstream AIRS Level 2 retrieval products, including atmospheric temperature profile, water vapor profile, surface temperature and surface emissivity, and a CH_4 first guess profile are used as the initial atmospheric state inputs to the forward Radiative Transfer Algorithm (RTA) (Strow et al., 2003) to compute the upwelling radiance in the pre-selected CH_4 absorption channels. The difference between the computed radiance and the associated AIRS Level 2 cloud cleared radiance product, ΔR, is represented in a linear approximation to the change in the CH_4 profile in percentage, ΔX, as follows:

$$\Delta R_n = \boldsymbol{S}_{n,L} \cdot \Delta X_L + \varepsilon, \quad (1)$$

where R_n is the cloud cleared radiance (observed), and ΔR_n is R_n minus the RTA calculated radiance in channel n, ΔX_L is the difference of CH_4 from the first guess at layer L that will be derived, and $\boldsymbol{S}_{n,L}$ is a vector of the sensitivities of radiance in channel n to changes ΔX_L in the CH_4 profile at L different levels, and ε is the error. For trace gas retrievals, a percentage or logarithmic perturbation to the trace gas abundance is used because Eq. (1) is more linear using this formulation than using an absolute difference in gas abundance. The ΔX_L is obtained by solving the Eq. (1) using singular value decomposition (SVD), and damping the least significant eigenfunctions of the SVD to constrain the solution. Similar algorithm was also used for the retrieval of nitrous Oxide

AMTD
8, 8563–8597, 2015

(N_2O), and more detail description of this algorithm for trace gases retrieval can be found in Xiong et al. (2008, 2014).

The major improvements in AIRS-V6 CH_4 retrieval algorithm include an increase in the number of retrieval layers, selection of more optimum channels, setting of damping parameter to constrain the retrieval, and small changes in the RTA regarding to the tuning of CH_4 absorption coefficients in the peak absorption channels near 7.66 µm. Compared to AIRS-V5 with seven retrieval layers, 10 vertically overlapping trapezoidal functions are used in AIRS-V6, as shown in Fig. 1, and the pressure levels are listed in Table 1. There are about 200 AIRS channels spanning the 7.66 µm CH_4 absorption band, of which 63 used in the AIRS-V6 CH_4 retrieval. In AIRS-V5, a 2 % increase in methane absorption coefficients for strong absorption channels near 1306 cm^{-1} was implemented (Xiong et al., 2008), and in V6 this adjustment was updated to 1–2 % for these peak channels. The damping parameter was then optimized after the increase of retrieval layers and re-selection of channels. The CH_4 first guess profile ("a priori") is similar to that in Version 5, which is a function of latitude and pressure (to capture its strong latitudinal and vertical gradients), and was generated through a non-linear polynomial fitting (Xiong et al., 2008).

2.2 AIRS sensitivity and the averaging kernels

The averaging kernels are defined to provide a simple characterization of the relationship between the retrieval and the true state, and the retrieval sensitivity can be illustrated from the sum of the columns of the averaging kernel matrix, which is also referred to as "the area of the averaging kernel" (Rodgers, 2000). As an example, Fig. 2 shows the averaging kernels for the 10 trapezoidal functions in the high northern latitude and in the tropics in September 2009. The averaging kernels corresponding to these 10 functions are broad and exhibit significant overlap, indicating that the retrieved amounts of CH_4 at different layers are not independent. The degrees of freedom (DOF), defined as the fractional number of significant eigenfunctions used in the retrieval process and computed as the trace of the averaging kernel matrix, is about 1.1 in the

AMTD
8, 8563–8597, 2015

tropics and 0.9 in the high northern hemisphere in this case. In general, the DOF in the tropics is higher than in the high latitudes, and the summer DOF is higher than the winter DOF.

To better see the retrieval sensitivity and its variation as a function of latitude and season, Fig. 3 shows the zonal averaged peak sensitive layer using two days' global data on 30 March 2010 and 1 July 2010. The peak sensitive layer in the tropics is between 100–500 hPa and has little seasonal variation. In the mid-latitude regions, the peak sensitive layer is between 200–600 hPa in March and rises to higher altitude at 150–600 hPa in July due to the enhanced water vapor in the atmosphere in summer time. The sensitive layer also depends on the thermal contrast. In the high northern hemisphere (60–90° N), the peak sensitive layer in March is between 300–600 hPa and rises to a slightly higher altitude in July as the water vapor is less than in the tropics.

3 Validation to AIRS-V6 CH_4 product

3.1 Data of aircraft measurement profiles used for validation

Table 2 lists the in-situ aircraft campaigns whose measured CH_4 profiles are used for validations in this paper. Figure 4 shows their spatial locations on the globe. Except for the HIPPO campaigns, measurements are mostly located over North America. More details of these campaigns are described as follows:

1. The Intercontinental Chemical Transport Experiment (INTEX) part A field mission was conducted in the summer of 2004 (1 July–15 August 2004) over North America (NA) and the Atlantic. This effort had a broad scope to investigate the transport and chemistry of long-lived greenhouse gases, oxidants and their precursors, aerosols and their precursors, as well their relationship with radiation and climate. NASA's DC-8 and J-31 were joined by aircraft from a large number of European and North American partners to explore the composition of the troposphere over NA and the Atlantic as well as radiative properties and effects of

AMTD
8, 8563–8597, 2015

clouds and aerosols in a coordinated manner (Simpson et al., 2002). An air sample is collected in different altitudes using a conditioned, evacuated 2-L stainless steel canister equipped with a bellows valve, and is returned to the UC-Irvine laboratory for CH_4 analysis using gas chromatography (GC, HP-5890A) with flame ionization detection. The use of the primary CH_4 calibration standards dating back to late 1977 ensures that these measurements are internally consistent. The measurement accuracy is ±1 % and the analytical precision at atmospheric mixing ratios is about 1 ppbv (Simpson et al., 2002, 2006).

2. INTEX-B was a major NASA led multi-partner atmospheric field campaign completed in the spring of 2006 (http://cloud1.arc.nasa.gov/intex-b/). INTEX-B was performed in two phases. In its first phase (1–21 March), INTEX-B operated as part of the Megacity Initiative: Local And Global Research Observations (MILAGRO) campaign with a focus on observations over Mexico and the Gulf of Mexico. In the second phase (17 April–15 May), the main INTEX-B focus was on trans-Pacific Asian pollution transport. Multiple airborne platforms carrying state of the art chemistry and radiation payloads were flown in concert with satellites and ground stations during the two phases of INTEX-B (Singh et al., 2009). The CH_4 aircraft measurements in INTEX-B are similar to INTEX-A.

3. The Arctic Research of the Composition of the Troposphere from Aircraft and Satellites (ARCTAS) mission was conducted in April and June–July 2008 by the Global Tropospheric Chemistry Program and the Radiation Sciences Program of NASA. Its objective was to better understand the factors driving current changes in Arctic atmospheric composition and climate. Three research aircrafts (DC-8, P-3, B-200) were used and a total of 24 research flights had been made. The aircraft were based in Alaska in April (ARCTAS-A) and in western Canada in June–July (ARCTAS-B). The DACOM instrument used is an infrared tunable diode laser absorption spectrometer which makes measurements of CH_4 (as well as CO and N_2O) at a 1 Hz sample rate. The CH_4 accuracy is tied to NOAA's Earth System

AMTD
8, 8563–8597, 2015

Research Laboratory, Global Monitoring Division (NOAA/ESRL/GMD) carbon cycle group standards and is nominally 1 %, and the precision is 0.1 % (1 sec, 1σ). CH_4 observations during ARCTAS-A showed little variability and no indication of significant April emissions from Arctic ecosystems. The July observations in ARCTAS-B over the Hudson Bay Lowlands revealed higher wetland emissions of methane than previously recognized (Jacob et al., 2010).

4. Aircraft measurements of the CH_4 vertical profiles were also made by the NOAA/ESRL Alaska Coast Guard (ACG) flight, in which CH_4 was measured with a Cavity Ringdown Spectroscopy (CRDS) analyzer at 0.4 Hz frequency with an overall measurement uncertainty of 2 ppb (Karion et al., 2012 and the references therein). ACG data in 2009, 2010 and 2011 were used and these data were provided by NOAA/ESRL/GMD.

5. Aircraft measurements of the CH_4 vertical profiles by the HIAPER Pole-to-Pole Observations (HIPPO) program over the Pacific Ocean (Wofsy et al., 2011) provide a unique dataset for validation over a wide latitudinal range (67° S–85° N). The National Science Foundation's Gulfstream V (GV) were used during all the five HIPPO missions. The GV transected the Pacific Ocean from 85° N to 67° S, performing in-progress vertical profiles every 220 km or 20 min (Wofsy et al., 2011, 2012). CH_4 was measured with a Quantum Cascade Laser Spectrometer (QCLS) at 1 Hz frequency with accuracy of 1.0 ppb and precision of 0.5 ppb (Kort et al., 2012). HIPPO methane data are reported on the NOAA04 calibration scale. The NOAA04 scale was designated as the official calibration scale, and consists of 16 gravimetrically prepared primary standards covering the nominal range of 300–2600 nmol mol^{-1}. This makes it suitable for use in calibrating standards for the measurement of air extracted from ice cores and contemporary measurements from GAW sites. This new scale results in CH_4 mole fractions that are a factor of 1.0124 greater than the previous scale (now desig-

AMTD
8, 8563–8597, 2015

nated CMDL83) (Dlugokencky et al., 2005). HIPPO data was downloaded from (http://hippo.ornl.gov/dataaccess).

3.2 Validation method

For each aircraft measurement profile, we calculated the mean location (latitude and longitude) and time. All AIRS retrievals (with quality flag equal to 0, 1) coincident with each aircraft profile within 200 km and from the same day were used to compute the mean retrieved profile, which is then compared with the corresponding aircraft profile smoothed after applying the averaging kernels as follows:

$$\hat{x} = \mathbf{A}x + (\mathbf{I} - \mathbf{A})\,x_a, \tag{2}$$

where $\mathbf{I}$ is the identity matrix, $\mathbf{A}$ is the averaging kernel matrix, x_a is the first guess profile (unit: part per billion, ppb), x is the in situ aircraft measurement profile, and the computed value $\hat{x}$, referred to as the convolved data later in this paper, will be compared with the retrieved CH_4 mixing ratio. As the aircraft profiles do not span the entire vertical range defined by the averaging kernels, extension of the aircraft profiles is required when using Eq. (2). This can be done using output from a chemistry model or climatology data to represent CH_4 mixing ratios in the upper troposphere and higher levels. In this paper we used the monthly averaged CH_4 data in 2007 from an Atmospheric General Circulation Model (AGCM)-based chemistry transport model (hereinafter ACTM) (Patra et al., 2011) to extrapolate from the ceiling of the aircraft profile to the top of atmosphere and from the lowest measurement height to the bottom of the atmosphere. The profile is then mapped to the 100 levels grid of RTA (Strow et al., 2003). The aircraft profiles with their ceilings beneath the 350 hPa pressure level were not used in validation.

The averaging kernels for each retrieved profile are applied to the same collocated aircraft data, and the mean of these convolved profiles is compared with the mean of the collocated retrieved profiles.

AMTD
8, 8563–8597, 2015

3.3 Optimization of quality control

The AIRS retrievals with quality flag equal to 0, 1 are usually counted as "good quality" retrievals and recommended to use. However, from the comparison with aircraft measurements we found some "good quality" retrieval profiles (with QC = 0, 1) show obvious oscillation. For example, Fig. 5 shows AIRS retrievals collocated with HIPPO-2 measurement at the location of (82.43° N, 150.4° W) in 21 November 2009. All the retrievals with quality flag as 0 and 1 within 150 km from aircraft measurements are shown in Fig. 5. However, two blue profiles show a big "bump" of over 1950 ppb at 400 hPa but a low value of about 1800 ppb near the surface. Considering CH_4 is well mixed in the mid-lower troposphere, these two profiles show obvious oscillation as opposed to the aircraft measurement and the first-guess. These two profiles are not as good as we expected, and we think the qualities of these profiles should be marked as "not good" and need to reset their quality flags to 2.

From the experiences we learned from this validation study, the quality flag for a retrieved profile that has the quality flag as 0 or 1 but does not pass the following two tests needs to reset to 2:

1. Oscillation test: for CH_4 mixing ratio between 350 and 50 hPa above the surface, if (the maximum–the mean) and (the minimum–the mean) are in opposite signs and its difference (the maximum–the minimum) is 5 % larger than the mean.

2. Strong inversion: the maximum CH_4 mixing ratio at ~ 400 hPa is 150 ppb (< 65° N) or 250 ppb (> 65° N) higher than the mixing ratio near the surface.

The profiles (with quality flag as 0 or 1) failed in either test are not recommended for use. However, we found the number of these profiles is only a small portion (less than 5 % in the cases we examined) of the total profiles with quality flag equal to 0 or 1, so for statistic analysis of computing mean CH_4 using more than hundreds of profiles in a large region, the error resulted from these bad quality profiles is estimated to be

AMTD
8, 8563–8597, 2015

insignificant. In this paper, the above optimized quality control was used to filter out some bad quality profiles.

4 Results and discussion

4.1 Validation results

Figure 6a shows the mean bias and RMS error of the retrieval in 100 levels using 941 aircraft profiles from nine campaigns. For comparison the error of the firstguess profile is also plotted. Below 400 hPa the bias is less than 0.5 % and RMS error is less than 1.5 %, and, as expected, the retrieval error as compared to the smoothed aircraft measurements is smaller than the direct comparison without applying the averaging kernels. From the information of the number of the aircraft measurements (Fig. 6b) we can see that the number of samples above 300 hPa is much less, so most profiles need to be extrapolated to the top of atmosphere using model data. This is why the retrieval bias and RMS error at above 300 hPa are even larger than the error of the first guess. This result also suggests that the first guess used in AIRS-V6 retrievals is good to represent the mean of climatology. Here we did not use the subset of samples with aircraft measurements above 300 hPa to compute the error separately considering: (1) the match-up was based on the mean latitude/longitude of the whole profile of aircraft measurement; (2) some profiles have measurements above 300 hPa but do not have enough measurements at lower levels; (3) the impact of stratospheric intrusion could exist to some profiles (Xiong et al., 2013b).

Further comparison between AIRS retrievals with collocated aircraft measurements in four trapezoid layers of 272–343, 343–441, 441–575 and 575–777 hPa are given in Fig. 7. Overall, the correlation between the AIRS retrievals and the aircraft measurements is very good ($R = 0.73 - 0.95$). A larger negative bias was found in upper layers, particularly when the CH_4 mixing ratio is lower than 1780 ppb. Compared with first guess, the retrieval error in the layers of 272–343 hPa (the upper left panel) is

AMTD
8, 8563–8597, 2015

even larger, but the retrieval errors in other layers are less than first guess and the correlations are improved, demonstrating the right work did by the retrievals.

To check the performance of the retrievals in different time and location, the retrieval error of CH_4 at layer 441–575 hPa is analyzed using the validation data in different seasons (Fig. 8) and different latitude zones (Fig. 9). It is evident that a larger negative bias of the retrievals occurs in the spring (March–May) (Fig. 8) and in the high northern hemisphere (60–90° N) (Fig. 9). While the CH_4 mixing ratio is lower than 1800 ppb, there is a negative bias during the summer (June–August) (Fig. 8) and mainly in the tropics (Fig. 9). From the correlation coefficient between AIRS retrievals and aircraft measurements, we found that, overall, a little worse correlation occurs in the mid-latitude region (30–60° N) (lower left panel in Fig. 9). The aircraft measurements used for validation in the mid-latitude region were mostly made over the North America, so the latitudinal gradient of CH_4 mixing ratio in this latitude zone (30–60° N) is small as compared to that in other latitude zones with an interval of 60°, which is part of reason why the correlation between the retrievals and aircraft measurements is relatively smaller.

4.2 Error analysis

There are quite a few sources contributing to the retrieval errors. First is the error from the radiative transfer model, particularly the uncertainty in spectroscopy of CH_4 absorption and line mixing. Recent study by Alvarado et al. (2015) showed the updates to the spectroscopic parameters for CH_4 resulted in a substantially smaller mean bias in the retrieved CH_4 when compared with HIPPO observations. Some correction of 1–2 % to the absorption coefficients was implemented for the strong CH_4 absorption channels which are near 1306 micron and mostly sensitive to high altitude (Xiong et al., 2008), but this correction is empirical and will need improvement in the RTA. Next is the error propagation since the CH_4 retrieval is based on the retrievals of atmospheric temperature and water moisture profiles, surface temperature and emissivity, so good retrievals in the upstream products will significantly impact to the retrieval of CH_4. Some

AMTD
8, 8563–8597, 2015

estimation of error propagation can be found from Xiong et al. (2008) and will not repeat here again. The third one is the lack of in-situ observations in layers above 300 hPa and the miss-match of AIRS observation with aircraft data in time and space domain. Even though the error due to the time difference is expected to be small over ocean (Wecht et al., 2012), but over land or in regions close to emission sources, this error will be much larger. So, better collocated aircraft measurements with satellite observations will be greatly helpful for satellite validations.

Here we just examined the relationships of the retrieval errors with latitude, DOFs and cloud fraction. As shown in Fig. 10, the mean bias is small and decreases from the southern hemisphere to mid-latitude of northern hemisphere, but the bias in the high northern hemisphere above 60° N is obviously larger than in the mid-latitude below 50° N. Also, the retrieval biases in the high latitude regions have a larger variability than in the tropics. From the upper right panel we can see the DOFs are mostly between 1.2–1.4 in the tropics, and 0.6–0.8 in the high northern latitude (above 60° N), and for DOFs >1.2 the biases are mostly positive. The biases are well correlated with the DOFs in the tropics (30° S–30° N, $R = 0.74$), but this correlation is much smaller in the mid-high latitude regions ($R = 0.36$, upper right panel). We also found that among different seasons the best correlation occurred in the summer. From the lower left panel, it is evident that most retrievals have a positive bias under clear sky, and in the tropics the biases have a negative-correlation with the cloud fractions (30° S–30° N, $R = -0.6$). We also found these positive biases under clear sky are largely found in the summer and fall, and the correlation of the bias with the cloud fraction in the summer is better than in other seasons. The correlation between the bias and cloud cover fraction is small in the mid-high latitude regions.

Further analysis (lower right panel) indicates the DOFs is negative-correlated with cloud fraction, and on average the correlation coefficient is $R = -0.7$ in the tropics and $R = -0.5$ in other regions. We also found that among different seasons the largest one is in the summer with $R = -0.8$ and -0.7 in the tropics and other regions respectively (not shown).

AMTD
8, 8563–8597, 2015

It has been a concern that the retrievals may be impacted by clouds since the cloud-cleared radiances are used in the retrievals. Our analysis found the correlation of the retrieval error with the DOFs is greater than the correlation with cloud cover fraction, suggesting that the dominant factor to the retrieval is the DOF. Examination to the correlation between DOFs and retrieval errors for different cloud fractions shows that under clear sky, the correlation coefficient is $R = 0.7$ (for cloud amount < 0.1), and it decreases to $R = 0.28$ for cloud amount > 0.5.

The correlation of retrieval error with cloud amount suggests the error in the cloud-cleared radiance is one important error source, and further improvement to the cloud-clearing algorithm is required in the future. These results also imply that the "observed" spatiotemporal variation by AIRS not only reflects the real change of CH_4 in the atmosphere, but also include some artificial impact from sensitivity, or DOF, and/or contamination by cloud. So, for the analysis of CH_4 distribution and/or seasonal variation using the retrieval products from AIRS (same for other thermal infrared sensors), some filtering of the data based on the DOFs and/or cloud amounts will help to remove part of this artificial variation; however, it is impossible to completely remove their impact to get the real spatiotemporal variation of CH_4 accurately based on the retrieved CH_4 mixing ratios only.

5 Summary and conclusion

Significant improvements in the CH_4 retrieval algorithm in AIRS-V6 was made, which include the increase of the retrieval layers from 6 to 10, reselect of channels and the adjustment of damping parameter. As a result, the peak sensitive layer near the tropics is between 100–500 and 200–600 hPa in the mid-high latitude regions, and the DOFs are mostly between 1.2–1.4 in the tropics, and 0.6–0.8 in the high northern latitude (above 60° N). In this paper, a thorough validation to AIRS-V6 CH_4 using about 1000 aircraft profiles from different campaigns was presented. In our validation the mean of AIRS retrievals within 200 km from each aircraft measurement and in the same day

AMTD
8, 8563–8597, 2015

was compared to the aircraft measurement after applying the averaging kernels. From these comparisons we found some optimization to the quality filtering of AIRS retrievals is desirable. Even though the population of these profiles is a small fraction (less than 5 %) of the total number retrieval profiles from the cases we examined, and its impact is estimated to be small for statistical analysis using hundreds of profiles in a large region, it is better to double-check the fraction of these profiles with inappropriate qualities and decide whether it is necessary to use the optimized quality flag suggested in this paper.

Validation results show that, on average, at layers 343–441 and 441–575 hPa the retrieval biases are −0.76 and −0.05 % with the RMS errors of 1.56 and 1.16 %, respectively. The bias of AIRS CH_4 is negative in high altitude and is much larger than in the lower altitude. The mean error in layer above 300 hPa is even larger than first guess, which is mainly due to the extrapolation of aircraft measurements to the top of atmosphere.

Further analysis of the retrieval errors with cloud fraction and the DOFs show the retrieval bias is well correlated with the DOF, especially when DOF is greater than 0.8. The correlation coefficient in the tropics is larger than in other regions, and in the summer is larger than in other seasons. We found the retrieval error is correlated with cloud cover when the cloud cover is less than 0.5. From the correlation between the DOF and cloud cover fraction, we conclude that the retrieval error is largely impacted by the DOF. This finding implies that the "observed" spatiotemporal variations by AIRS and/or other thermal infrared sensors not only reflect the real change of CH_4 in the atmosphere, but also include some artificial impact from the sensors and the retrieval sensitivity. Considering the change of DOF in different latitudes and different seasons (Fig. 3), we suggest that for data analysis some filtering of the data based on the DOFs and/or cloud amounts will help to remove part of this artificial variation.

Acknowledgements. This research was supported by funding from NOAA Office of Application & Research. The data used in this effort were acquired as part of the activities of NASA's Science Mission Directorate, and are archived and distributed by the Goddard Earth Sciences

AMTD
8, 8563–8597, 2015

(GES) Data and Information Services Center (DISC). The aircraft measurement data is from HIAPER Pole-to-Pole Observations (HIPPO) program.

The views, opinions, and findings contained in this paper are those of the authors and should not be construed as an official National Oceanic and Atmospheric Administration or US Government position, policy, or decision.

References

Alvarado, M. J., Payne, V. H., Cady-Pereira, K. E., Hegarty, J. D., Kulawik, S. S., Wecht, K. J., Worden, J. R., Pittman, J. V., and Wofsy, S. C.: Impacts of updated spectroscopy on thermal infrared retrievals of methane evaluated with HIPPO data, Atmos. Meas. Tech., 8, 965–985, doi:10.5194/amt-8-965-2015, 2015.

Aumann, H. H., Chahine, M. T., Gautier, C., Goldberg, M. D., Kalnay, E., McMillin, L. M., Revercomb, H., Rosenkranz, P. W., Smith, W. L., Staelin, D. H., Strow, L. L., and Susskind, J.: AIRS/AMSU/HSB on the aqua mission: Design, science objectives, data products, and processing systems. IEEE Trans. Geosci. Remote Sens., 41, 253–264, 2003.

Bergamaschi, P., Houweling, H., Segers, A., Krol, M., Frankenberg, C., Scheepmaker, R. A., Dlugokencky, E., Wofsy, S. C., Kort, E. A., Sweeney, C., Schuck, T., Brenninkmeijer, C., Chen, H., Beck, V., and Gerbig, C.: Atmospheric CH_4 in the first decade of the 21st century: Inverse modeling analysis using SCIAMACHY satellite retrievals and NOAA surface measurements, J. Geophys. Res. Atmos., 118, 7350–7369, doi:10.1002/jgrd.50480, 2013.

Bousquet, P., Ciais, P., Miller, J. B., Dlugokencky, E. J., Hauglustaine, D. A., Prigent, C., van der Werf, G. R., Peylin, P., Brunke, E. G., Carouge, C., Langenfelds, R. L., Lathière, J., Papa, F., Ramonet, M., Schmidt, M., Steele, L. P., Tyler, S. C., and White, J.: Contribution of anthropogenic and natural sources to atmospheric methane variability, Nature, 443, 439–443, doi:10.1038/nature05132, 2006.

Bousquet, P., Ringeval, B., Pison, I., Dlugokencky, E. J., Brunke, E.-G., Carouge, C., Chevallier, F., Fortems-Cheiney, A., Frankenberg, C., Hauglustaine, D. A., Krummel, P. B., Langenfelds, R. L., Ramonet, M., Schmidt, M., Steele, L. P., Szopa, S., Yver, C., Viovy, N., and Ciais, P.: Source attribution of the changes in atmospheric methane for 2006–2008, Atmos. Chem. Phys., 11, 3689–3700, doi:10.5194/acp-11-3689-2011, 2011.

AMTD
8, 8563–8597, 2015

Bruhwiler, L., Dlugokencky, E., Masarie, K., Ishizawa, M., Andrews, A., Miller, J., Sweeney, C., Tans, P., and Worthy, D.: CarbonTracker-CH4: an assimilation system for estimating emissions of atmospheric methane, Atmos. Chem. Phys., 14, 8269–8293, doi:10.5194/acp-14-8269-2014, 2014.

Chen, Y.-H. and Prinn, R. G.: Estimation of atmospheric methane emissions between 1996 and 2001 using a three-dimensional global chemical transport model, J. Geophys. Res., 111, D10307, doi:10.1029/2005jd006058, 2006.

Crevoisier, C., Nobileau, D., Fiore, A. M., Armante, R., Chédin, A., and Scott, N. A.: Tropospheric methane in the tropics – first year from IASI hyperspectral infrared observations, Atmos. Chem. Phys., 9, 6337–6350, doi:10.5194/acp-9-6337-2009, 2009.

Crevoisier, C., Nobileau, D., Armante, R., Crépeau, L., Machida, T., Sawa, Y., Matsueda, H., Schuck, T., Thonat, T., Pernin, J., Scott, N. A., and Chédin, A.: The 2007–2011 evolution of tropical methane in the mid-troposphere as seen from space by MetOp-A/IASI, Atmos. Chem. Phys., 13, 4279–4289, doi:10.5194/acp-13-4279-2013, 2013.

Dlugokencky, E. J., Myers, R. C., Lang, P. M., Masarie, K. A., Crotwell, A. M., Thoning, K. W., Hall, B. D., Elkins, J. W., and Steele, L. P.: Conversion of NOAA atmospheric dry air CH4 mole fractions to a gravimetrically prepared standard scale, J. Geophys. Res., 110, D18306, doi:10.1029/2005JD006035, 2005.

Frankenberg, C., Bergamaschi, P., Butz, A., Houweling, S., Meirink, J. F., Notholt, J., Petersen, A. K., Schrijver, H., Warneke, T., and Aben, I.: Tropical methane emissions: A revised view from SCIAMACHY onboard ENVISAT, Geophys. Res. Lett., 35, L15811, doi:10.1029/2008GL034300, 2008.

Frankenberg, C., Aben, I., Bergamaschi, P., Dlugokencky, E. J., van Hees, R., Houweling, S., van der Meer, P., Snel, R., and Tol, P.: Global column-averaged methane mixing ratios from 2003 to 2009 as derived from sciamachy: Trends and variability, J. Geophys. Res., 116, D04302, doi:10.1029/2010jd014849, 2011.

Jacob, D. J., Crawford, J. H., Maring, H., Clarke, A. D., Dibb, J. E., Emmons, L. K., Ferrare, R. A., Hostetler, C. A., Russell, P. B., Singh, H. B., Thompson, A. M., Shaw, G. E., McCauley, E., Pederson, J. R., and Fisher, J. A.: The Arctic Research of the Composition of the Troposphere from Aircraft and Satellites (ARCTAS) mission: design, execution, and first results, Atmos. Chem. Phys., 10, 5191–5212, doi:10.5194/acp-10-5191-2010, 2010.

AMTD
8, 8563–8597, 2015

Karion, A., Sweeney, C., Wolter, S., Newberger, T., Chen, H., Andrews, A., Kofler, J., Neff, D., and Tans, P.: Long-term greenhouse gas measurements from aircraft, Atmos. Meas. Tech. Discuss., 5, 7341–7382, doi:10.5194/amtd-5-7341-2012, 2012.

Kirschke, S., Bousquet, P., Ciais, P., Saunois, M., Bergamaschi, P., Bruhwiler, L., Canadell, J. G., Chevallier, F., Dlugokencky, E. J., Feng, L., Fraser, A., Heimann, M., Hodson, E., Houweling, S., Josse, B., Lamarque, J.-F., Quéré, C. L., Nagashima, T., Naik, V., Palmer, P., Pison, I., Poulter, B., Ringeval, B., Shindell, D. T., Spahni, R., Strode, S. A., Szopa, S., van der Werf, G. R., Voulgarakis, A., and Zeng, G.: Three decades of methane sources and sinks: budgets and variations, Nat. Geosci., 6, 813–823, 2013.

Kort, E. A., Wofsy, S. C., Daube, B. C., Diao, M., Elkins, J. W., Gao, R. S., Hintsa, E. J., Hurst, D. F., Jimenez, R., Moore, F. L., Spackman, J. R., and Zondlo, M. A.: Atmospheric observations of Arctic Ocean methane emissions up to 82° north, Nat. Geosci., 5, 318–321, doi:10.1038/ngeo1452, 2012.

Maddy, E. S., DeSouza-Machado, S. G., Nalli, N. R., Barnet, C. D., L Strow, L., Wolf, W. W., Xie, H., Gambacorta, A., King, T. S., Joseph, E., Morris, V., Hannon, S. E., and Schou, P: On the effect of dust aerosols on AIRS and IASI operational level 2 products, Geophys. Res. Lett., 39, L10809, doi:10.1029/2012GL052070, 2012.

Massart, S., Agusti-Panareda, A., Aben, I., Butz, A., Chevallier, F., Crevoisier, C., Engelen, R., Frankenberg, C., and Hasekamp, O.: Assimilation of atmospheric methane products into the MACC-II system: from SCIAMACHY to TANSO and IASI, Atmos. Chem. Phys., 14, 6139–6158, doi:10.5194/acp-14-6139-2014, 2014.

Meirink, J. F., Bergamaschi, P., and Krol, M. C.: Four-dimensional variational data assimilation for inverse modelling of atmospheric methane emissions: method and comparison with synthesis inversion, Atmos. Chem. Phys., 8, 6341–6353, doi:10.5194/acp-8-6341-2008, 2008.

Parker, R., Boesch, H., Cogan, A., Fraser, A., Feng, L., Palmer, P. I., Messerschmidt, J., Deutscher, N., Griffith, D. W. T., Notholt, J., Wennberg, P. O., and Wunch, D.: Methane observations from the Greenhouse Gases Observing SATellite: Comparison to ground-based TCCON data and model calculations, Geophys. Res. Lett., 38, L15807, doi:10.1029/2011GL047871, 2011.

Patra, P. K., Houweling, S., Krol, M., Bousquet, P., Belikov, D., Bergmann, D., Bian, H., Cameron-Smith, P., Chipperfield, M. P., Corbin, K., Fortems-Cheiney, A., Fraser, A., Gloor, E., Hess, P., Ito, A., Kawa, S. R., Law, R. M., Loh, Z., Maksyutov, S., Meng, L., Palmer, P. I., Prinn, R. G., Rigby, M., Saito, R., and Wilson, C.: TransCom model simulations of

AMTD
8, 8563–8597, 2015

CH4 and related species: linking transport, surface flux and chemical loss with CH4 variability in the troposphere and lower stratosphere, Atmos. Chem. Phys., 11, 12813–12837, doi:10.5194/acp-11-12813-2011, 2011.

Payne, V. H., Clough, S. A., Shephard, M. W., Nassar, R., and Logan, J. A.: Information-centered representation of retrievals with limited degrees of freedom for signal: Application to methane from the tropospheric emission spectrometer, J. Geophys. Res., 114, D10307, doi:10.1029/2008jd010155, 2009.

Razavi, A., Clerbaux, C., Wespes, C., Clarisse, L., Hurtmans, D., Payan, S., Camy-Peyret, C., and Coheur, P. F.: Characterization of methane retrievals from the IASI space-borne sounder, Atmos. Chem. Phys., 9, 7889–7899, doi:10.5194/acp-9-7889-2009, 2009.

Rodgers, C. D.: Inverse methods for atmospheric sounding: Theory and Practic, World Scientific Publishing Co. Pte. Ltd, Singapore, 2000.

Saitoh, N., Touno, M., Hayashida, S., Imasu, R., Shiomi, K., Yokota, T., Yoshida, Y., Machida, T., Matsueda, H., and Sawa, Y.: Comparisons between XCH4 from GOSAT Shortwave and Thermal Infrared Spectra and Aircraft CH_4 Measurements over Guam, SOLA, 8, 145–149, doi:10.2151/sola.2012-036, 2012.

Schepers, D., Guerlet, S., Butz, A., Landgraf, J., Frankenberg, C., Hasekamp, O., Blavier, J. F., Deutscher, N. M., Griffith, D. W. T., Hase, F., Kyro, E., Morino, I., Sherlock, V., Sussmann, R., and Aben, I.: Methane retrievals from Greenhouse Gases Observing Satellite (GOSAT) shortwave infrared measurements: Performance comparison of proxy and physics retrieval algorithms, J. Geophys. Res., 117, D10307, doi:10.1029/2012jd017549, 2012.

Simpson, I. J., Chen, T.-Y., Blake, D. R., and Rowland, F. S.: Implications of the recent fluctuations in the growth rate of tropospheric methane, Geophys. Res. Lett., 29, 1479, doi:10.1029/2001GL014521, 2002.

Simpson, I. J., Rowland, F. S., Meinardi, S., and Blake, D. R.: Influence of biomass burning during recent fluctuations in the slow growth of global tropospheric methane, Geophys. Res. Lett., 33, L22808, doi:10.1029/2006GL027330, 2006.

Singh, H. B., Brune, W. H., Crawford, J. H., Flocke, F., and Jacob, D. J.: Chemistry and transport of pollution over the Gulf of Mexico and the Pacific: spring 2006 INTEX-B campaign overview and first results, Atmos. Chem. Phys., 9, 2301–2318, doi:10.5194/acp-9-2301-2009, 2009.

Strow, L. L., Hannon, S. E., De Souza-Machado, S., Motteler, H. E., and Tobin, D. C.: An overview of the AIRS radiative transfer model, IEEE Trans. Geosci. Remote Sens., 41, 303–313, 2003.

AMTD
8, 8563–8597, 2015

Susskind, J., Blaisdell, J. M., Iredell, L., and Keita, F.: Improved temperature sounding and quality control methodology using AIRS/AMSU data: The AIRS Science Team version 5 retrieval algorithm, IEEE Trans. Geosci. Remote Sens., 49, 883–907, doi:10.1109/TGRS.2010.2070508, 2011.

Wecht, K. J., Jacob, D. J., Wofsy, S. C., Kort, E. A., Worden, J. R., Kulawik, S. S., Henze, D. K., Kopacz, M., and Payne, V. H.: Validation of TES methane with HIPPO aircraft observations: implications for inverse modeling of methane sources, Atmos. Chem. Phys., 12, 1823–1832, doi:10.5194/acp-12-1823-2012, 2012.

Wofsy, S. C., H. S. Team, T. Cooperating Modellers, and T. Satellite (2011), HIAPER Pole-to-Pole Observations (HIPPO): fine-grained, global-scale measurements of climatically important atmospheric gases and aerosols, Philos. T. Roy. Soc. A, 369, 2073–2086, doi:10.1098/rsta.2010.0313, 1943.

Wofsy, S. C., Daube, B. C., Jimenez, R., Kort, E., Pittman, J. V., Park, S., Commane, R., Xiang, B., Santoni, G., Jacob, D., Fisher, J., Pickett-Heaps, C., Wang, H., Wecht, K., Wang, Q.-Q., Stephens, B. B., Shertz, S., Watt, A. S., Romashkin, P., Campos, T., Haggerty, J., Cooper, W. A., Rogers, D., Beaton, S., Hendershot, R., Elkins, J. W., Fahey, D. W., Gao, R. S., Moore, F., Montzka, S. A., Schwarz, J. P., Perring, A. E., Hurst, D., Miller, B. R., Sweeney, C., Oltmans, S., Nance, D., Hintsa, E., Dutton, G., Watts, L. A., Spackman, J. R., Rosenlof, K. H., Ray, E. A., Hall, B., Zondlo, M. A., Diao, M., Keeling, R., Bent, J., Atlas, E. L., Lueb, R., and Mahoney, M. J.: HIPPO Merged 10-second Meteorology, Atmospheric Chemistry, Aerosol Data (R_20121129), Carbon Dioxide Information Analysis Center, Oak Ridge National Laboratory, Oak Ridge, Tennessee, USA, doi:10.3334/CDIAC/hippo_ 010, 2012.

Worden, J., Kulawik, S., Frankenberg, C., Payne, V., Bowman, K., Cady-Peirara, K., Wecht, K., Lee, J.-E., and Noone, D.: Profiles of CH_4, HDO, H_2O, and N_2O with improved lower tropospheric vertical resolution from Aura TES radiances, Atmos. Meas. Tech., 5, 397–411, doi:10.5194/amt-5-397-2012, 2012.

Xiong, X., Barnet, C., Maddy, E., Sweeney, C., Liu, X., Zhou, L., and Goldberg, M.: Characterization and validation of methane products from the Atmospheric Infrared Sounder (AIRS), J. Geophys. Res., 113, G00A01, doi:10.1029/2007JG000500, 2008.

Xiong, X., Barnet, C., Maddy, E., Wei, J., Liu, X., and Pagano, T. S.: Seven Years' Observation of Mid-Upper Tropospheric Methane from Atmospheric Infrared Sounder, Remote Sens., 2, 2509–2530, 10.3390/rs2112509, 2010.

AMTD
8, 8563–8597, 2015

Xiong, X., Barnet, C., Maddy, E. S., Gambacorta, A., King, T. S., and Wofsy, S. C.: Mid-upper tropospheric methane retrieval from IASI and its validation, Atmos. Meas. Tech., 6, 2255–2265, doi:10.5194/amt-6-2255-2013, 2013a.

Xiong, X., Barnet, C., Maddy, E., Wofsy, S. C., Chen, L., Karion, A., and Sweeney, C.: Detection of methane depletion associated with stratospheric intrusion by atmospheric infrared sounder (AIRS), Geophys. Res. Lett., 40, 2455–2459, doi:10.1002/grl.50476, 2013b.

Xiong, X., Maddy, E. S., Barnet, C., Gambacorta, A., Patra, P. K., Sun, F., and Goldberg, M.: Retrieval of nitrous oxide from Atmospheric Infrared Sounder: Characterization and validation, J. Geophys. Res. Atmos., 119, 9107–9122, doi:10.1002/2013JD021406, 2014.

Yokota. T., Yoshida, Y., Eguchi, N., Ota, Y., Tanaka, T., Watanabe, H., and Maksyutov, S.: Global Concentrations of CO_2 and CH_4, retrieved from GOSAT: First Preliminary Results, SOLA, 5, 160–163, 2009.

AMTD
8, 8563–8597, 2015

Table 1. AIRS Trapozoid Layers used in retrieval (hPa).

Level	1	2	3	4	5	6	7	8	9	10	11
hPa	0.016	11.0	103.0	160.5	212.0	272.9	343.6	441.9	575.5	777.8	1100.0

AMTD
8, 8563–8597, 2015

Table 2. A brief description of 9 campaigns used for validation.

Campaign name	Time (mm/year)	Number of profiles used
INTEX–A	07/2004	71
INTEX–B	03/2006–05/2006	61
ARCTAS	03/2008–07/2008	66
ACG	2009–2011	144
HIPPO–1	01/2009	108
HIPPO–2	10/2009–11/2009	128
HIPPO–3	03/2010–04/2010	114
HIPPO-4	06/2011–07/2011	116
HIPPO-5	08/2011–09/2011	133

AMTD
8, 8563–8597, 2015

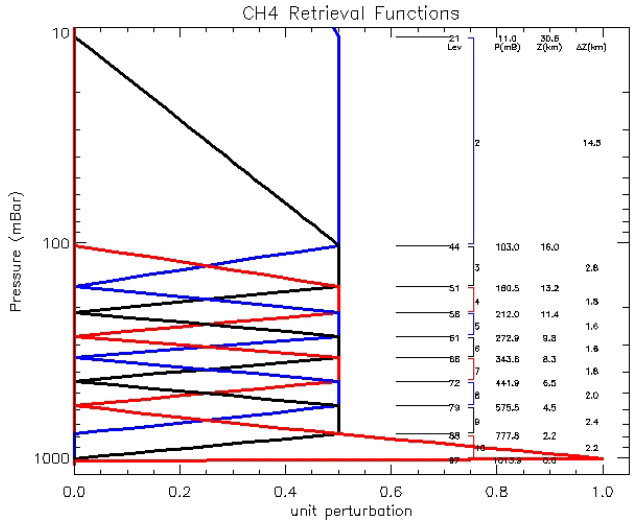

Figure 1. Ten Trapazoid functions used for CH_4 retrieval in AIRS-V6.

AMTD
8, 8563–8597, 2015

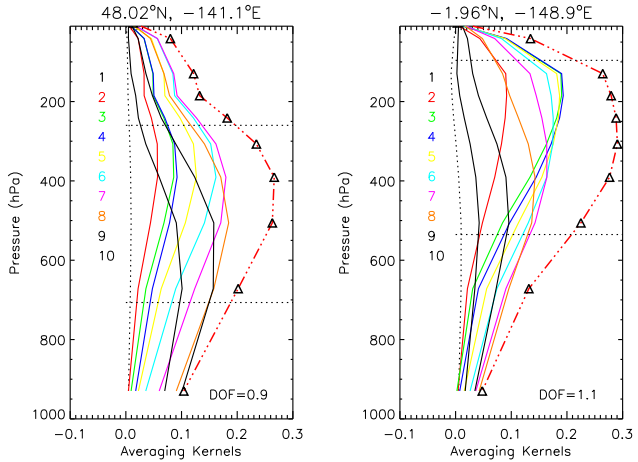

Figure 2. Examples of the averaging kernels in the high northern hemisphere and the tropics in September 2009. Different colors correspond to 10 different trapozoid functions (see Table 1). In order to plot the area of the averaging kernels in the same range of x axis, the red dash line is the area of the averaging kernels divided by 4. The peak sensitive layer is between the two black parallel dash lines, which are determined by the area of the averaging kernel that is equal to $1/\sqrt{2}$ of its maximum value.

AMTD
8, 8563–8597, 2015

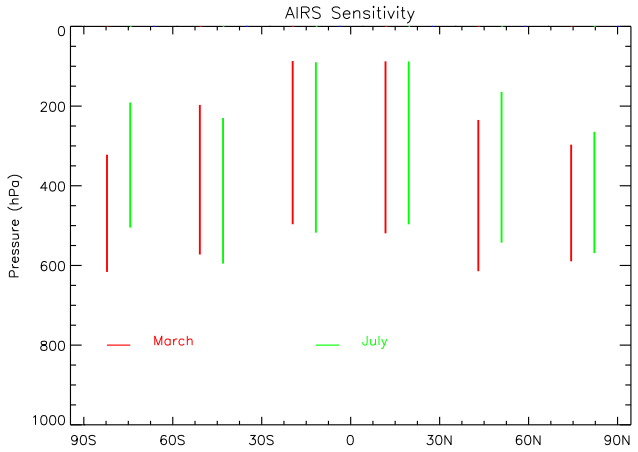

Figure 3. AIRS peak sensitive layers for six latitude zones with an interval of 30° (see Fig. 2 for the definition of the peak sensitive layer).

AMTD
8, 8563–8597, 2015

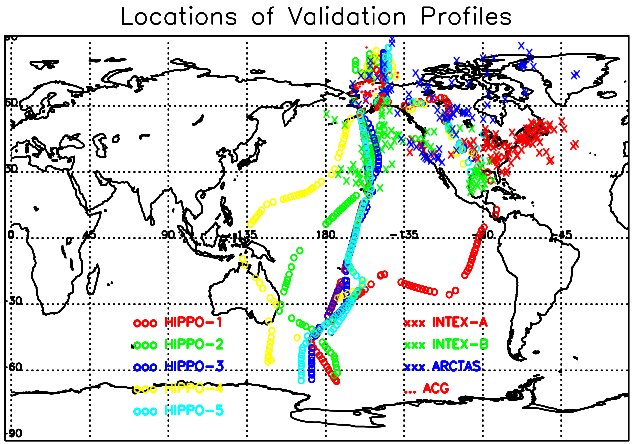

Figure 4. Locations of the aircraft measurement profiles used for validation. Different colors and symbols are for different campaigns.

AMTD
8, 8563–8597, 2015

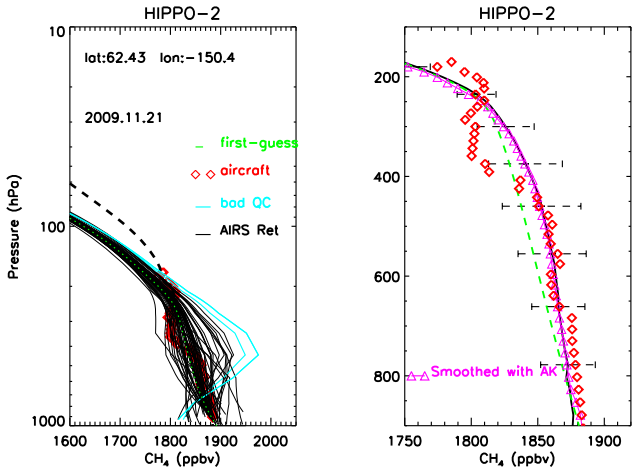

Figure 5. CH_4 profile on April 3, 2010 by HIPPO-3 aircraft measurement (red dots) vs all AIRS retrievals in a collocation window with a distance of 150 km and in the same day. The right panel is the mean profile of AIRS retrievals with the bars showing the standard deviation, the aircraft measurements smoothed with the averaging kernels (AK) (purple, triangles), and the first guess profile (green dash line).

AMTD
8, 8563–8597, 2015

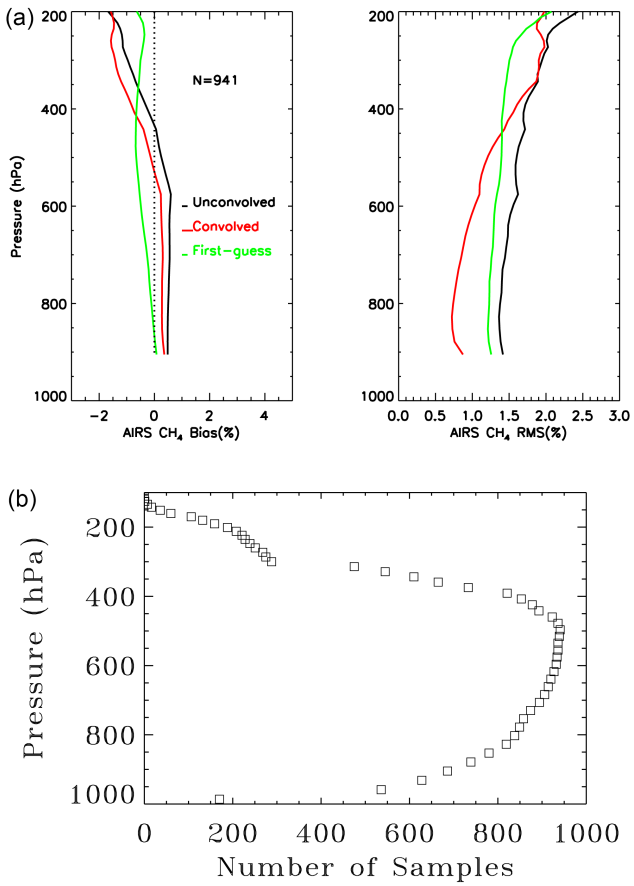

Figure 6. (a) Bias (left) and RMS errors (right) of the AIRS retrieved CH_4 mixing ratio and the first guess profile as compared to aircraft profiles (N = 941). **(b)** Number of samples of aircraft measurements in different altitudes.

AMTD
8, 8563–8597, 2015

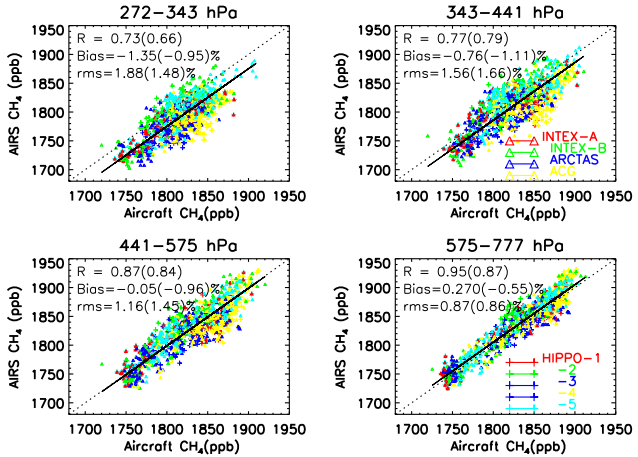

Figure 7. AIRS-V6 retrieved CH_4 mixing ratio compared to collocated aircraft profiles from different campaign in four trapezoid layers of 272–343, 343–441, 441–575 and 575–777 hPa. *x* axis is the convolved aircraft measurements, and *y* axis is the mean of AIRS retrieved profiles within 200 km and in the same day of the measurement time and site location. Different colors are from different campaigns. The correlation coefficient (*R*) and the bias and RMS error (in percentage %) for both AIRS retrieval and the first-guess (inside parentheses) are given.

AMTD
8, 8563–8597, 2015

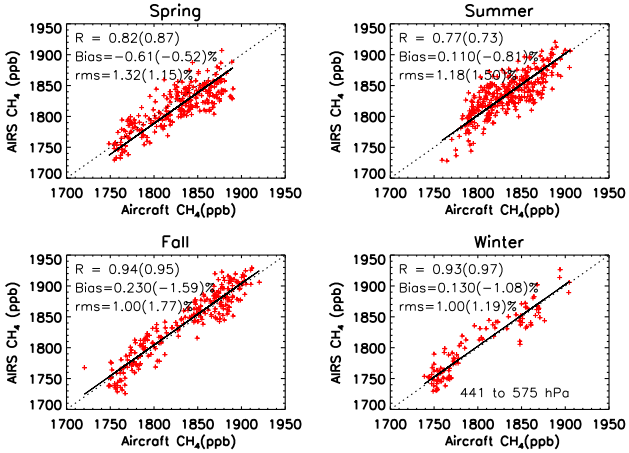

Figure 8. Similar to Fig. 7 but for the CH_4 at layer 441–575 hPa in four seasons.

AMTD
8, 8563–8597, 2015

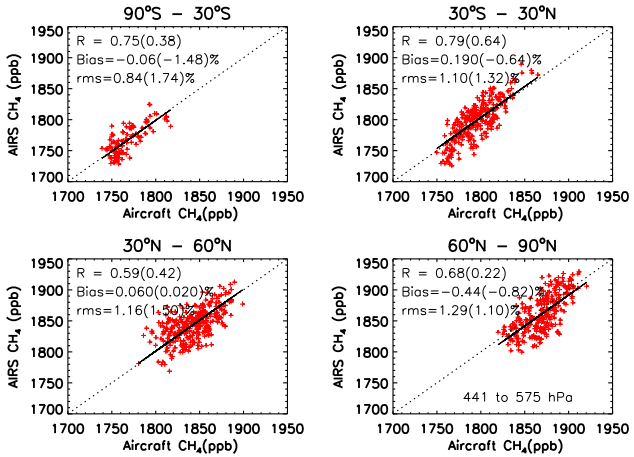

Figure 9. Same as Fig. 7 but for the CH_4 at layer 441–575 hPa in different latitude zones.

AMTD
8, 8563–8597, 2015

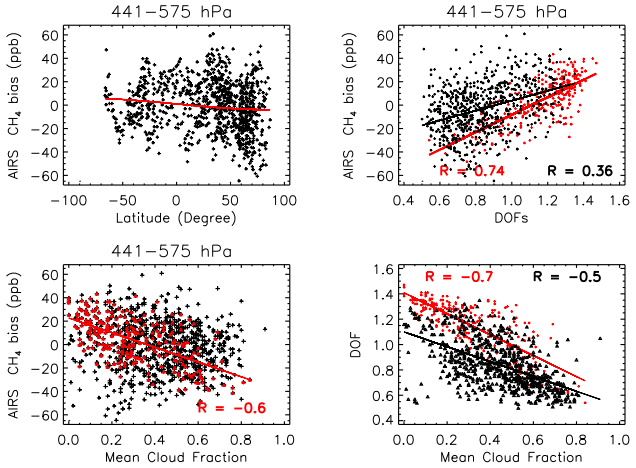

Figure 10. Variation of the AIRS CH_4 retrieval bias for layer 441-575 hPa with latitude, the mean degrees of freedom (DOFs) and cloud fraction, and the correlation between the mean DOF and cloud fraction. Upper left: red line is the linear fitting using all data.

AMTD
8, 8563–8597, 2015